energies

MDPI

Article

Investigation of Split Diesel Injections in Methanol/Diesel Dual-Fuel Combustion in an Optical Engine

Hongyi Zhang [1,†], Zhonghui Zhao [2,†], Jun Wu [1], Xinyan Wang [3], Weihao Ouyang [2] and Zhaowen Wang [2,*]

[1] School of Naval Architecture and Ocean Engineering, Huazhong University of Science and Technology, Wuhan 430074, China; u202112589@hust.edu.cn (H.Z.); wuj@hust.edu.cn (J.W.)
[2] School of Energy and Power Engineering, Huazhong University of Science and Technology, Wuhan 430074, China; lenovo2021zzh@outlook.com (Z.Z.); oywh2536@163.com (W.O.)
[3] Centre for Advanced Powertrain and Fuels, Brunel University London, Uxbridge UB8 3PH, UK; xinyan.wang@brunel.ac.uk
* Correspondence: wangzhaowen@hust.edu.cn
† These authors contributed equally to this work.

Abstract: Methanol is a promising alternative fuel due to its wide availability of raw materials, mature production processes, and low production cost. However, because of the low cetane number, methanol must include a more reactive fuel to assist with combustion when used in compression ignition (CI) engines. In this study, based on the optical CI engine platform, methanol is injected into the intake port, and diesel is directly injected into the cylinder to achieve dual-fuel combustion. The effects of the methanol energy ratios and diesel split injection strategies on combustion are investigated. The results show that the premixed blue flame was mainly concentrated in the near wall region, whereas the yellow flame produced by diesel combustion tended to concentrate in the central region as the methanol energy ratio increased. When the methanol energy ratio exceeded 50%, the ignition delay was significantly prolonged, while the flame area was greatly reduced. Meanwhile, the peak values for the cylinder pressure and heat release rate decreased significantly, indicating a significant deterioration in combustion. At the earlier diesel pre-injection timing at −58°, the overall dual-fuel combustion at each main injection timing exhibited low-temperature premixed combustion characteristics, with a lower peak exothermic rate and flame brightness. At the later pre-injection timing at −33°, the spray flame at all main injection timings could be observed, with higher peak heat release rates and indications of thermal efficiency. Combustion at later main injection timings was characterized by diffusion combustion, and the main injection timing could effectively regulate the combustion process through phase adjustment.

Keywords: optical engine; diesel/methanol; methanol energy ratio; main injection timing; combustion process

Citation: Zhang, H.; Zhao, Z.; Wu, J.; Wang, X.; Ouyang, W.; Wang, Z. Investigation of Split Diesel Injections in Methanol/Diesel Dual-Fuel Combustion in an Optical Engine. *Energies* **2024**, *17*, 3382. https://doi.org/10.3390/en17143382

Academic Editor: Anastassios M. Stamatelos

Received: 19 June 2024
Revised: 7 July 2024
Accepted: 8 July 2024
Published: 10 July 2024

1. Introduction

Compression ignition (CI) internal combustion engines are widely used in key areas such as ground transportation, power generation, and industrial production, owing to their unique advantages of reliability and high efficiency [1]. However, traditional CI engines have consumed large amounts of fossil fuels in their applications over the past several years, resulting in the emission of large amounts of soot, nitrogen oxides, and greenhouse gases [2–4]. Therefore, in recent years, prominent issues such as energy shortages, environmental pollution, and greenhouse effects have emerged in the world [5]. Finding clean alternative fuels and exploring efficient and clean combustion methods are the main means of solving these problems.

As a renewable low-carbon fuel, methanol is a promising alternative fuel, owing to its wide availability [6], mature production processes [7–9], and low cost. With a simple composition and no sulfur content, methanol produces only CO_2 and water when fully

burned. It contains 50% oxygen, which is beneficial for improving the mixture concentration and promoting combustion [10–12]. Additionally, because of the absence of carbon-carbon bonds in its composition, methanol produces virtually no soot during the combustion process [13], making it an ideal clean fuel. Under normal conditions, methanol is in a liquid state and only solidifies at the extremely low temperature of −89 °C, making it suitable for use in high-altitude and extremely cold regions. Its convenient storage and transportation provide favorable conditions for widespread application. Furthermore, methanol possesses excellent thermochemical properties, such as a high latent heat of vaporization, which helps air intake and reduces the combustion temperature, leading to lower thermal loads and reduced NOx emissions [14]. Additionally, its low minimum ignition energy and fast flame propagation speed facilitate complete combustion. With a high octane number, methanol is less likely to cause knocking when applied to an engine [15]. Therefore, methanol has attracted widespread research attention in recent years [16–18].

Owing to its faster combustion speed and gasoline-like properties [19], research on methanol has long focused on spark ignition engines. Nguyen et al. [20] studied the lean combustion of methanol in direct injection spark-ignition engines and found that under full throttle conditions, the limit of excess air coefficient (λ) for stable combustion of methanol is 1.5, which is higher than that of gasoline (1.2). Within the range of 1.2–1.4, the effective thermal efficiency increases with λ, while the opposite occurs at λ values beyond 1.4. Compared with gasoline, the use of methanol results in a higher mean effective pressure and a shorter ignition delay and combustion duration. Li et al. [21] studied the ignition effects of various preheating methods during a cold start in 2009 and found that the cylinder temperature has a significant impact on cold starting in methanol-fueled engines. Preheating methods such as preheating methanol and air cannot guarantee ignition, while preheating the intake manifold with resistance wire and a glow plug can ensure reliable ignition, with the glow plug providing better preheating effects. Subsequently, Li et al. [22] investigated the effects of the optimal injection and ignition timing on the performance of methanol engines. The results showed that under the full load range and an engine speed of 1600 rpm, optimized injection and spark ignition timing can reduce the effective fuel consumption rate by more than 10% and achieve a good balance between the indicated thermal efficiency and CO, THC, and NOx emissions. In addition, Li et al. [23] studied the combustion performance and emissions of gasoline-methanol, ethanol, and butanol blends (alcohol blending volume ratio of 10–60%) in port fuel injection (PFI) spark-ignition engines. They found that the combustion phase of each blended fuel occurred earlier than that of gasoline, but the effective thermal efficiency was lower. Compared with gasoline, the methanol-gasoline blends had increased unburned HC emissions, while the ethanol and butanol blends had fewer emissions. The methanol-gasoline blends had the fewest NOx emissions across different blending ratios. Nidhi et al. [24] explored the impact of the air oxygen content on the performance of methanol-fueled spark-ignition engines. The results showed that compared with the baseline oxygen content (23%), oxygen-rich air resulted in a higher effective thermal efficiency and increased constant-volume combustion. When using intake air with an oxygen content of 60.4%, the peak pressure increased more than twofold, whereas CO and HC emissions decreased by 48.6% and 30.9%, respectively. Additionally, as the oxygen content increased, NOx emissions were higher due to the temperature increase, but at an oxygen content of 60.4%, NOx emissions decreased sharply, owing to a reduction in the nitrogen content. These research results fully demonstrate the superiority of using methanol in spark-ignition engines, particularly in terms of improving lean combustion limits and reducing pollutant emissions.

The properties of methanol allow it to be operated in compression-ignition engines with higher compression ratios and burn more cleanly than diesel. Nevertheless, methanol is challenging to use in CI engines because of its low cetane number, which requires highly reactive fuel to assist combustion. Li et al. [25] studied the impact of diesel injection parameters on a diesel/methanol heavy-duty engine and found that increasing the diesel injection pressure increased the rapid combustion proportion, which could increase engine noise,

while advancing the diesel injection timing and increasing the injection mass decreased the rapid combustion proportion. Compared with pure diesel, the dual-fuel mode significantly increased CO and HC emissions but reduced NOx and soot emissions. Li et al. [26] conducted a numerical simulation study on the influencing factors of methanol/diesel combustion and found that the fuel proportion of methanol and the diesel injection timing determined the ignition starting and heat release processes by influencing the fuel reactivity distribution. Increasing the proportion of methanol and advancing the diesel injection timing are beneficial for fuel economy and for avoiding knocking. Increasing the initial temperature while increasing the proportion of methanol maintained a stable combustion phase and reduced almost all emissions. Tao et al. [27] studied the diesel pre-injection strategy for a methanol dual-fuel engine and found that the introduction of diesel pre-injection advanced the start of the combustion process and increased the peak heat release. Advancing the pre-injection timing increased the ignition delay and shortened the combustion duration, and NOx emissions first decreased and then increased. As the proportion of pre-injection diesel increased, the peak combustion pressure and heat release increased, NOx emissions increased, and soot emissions decreased. Under high methanol substitution ratios, advancing the pre-injection timing, increasing the pre-injection proportion, and being combined with EGR can achieve better combustion and emission performance for the engine. Liu et al. [28] conducted tests on pilot injection strategies under low loads and found that, compared with diesel single-stage injection, the addition of diesel pre-injection could increase the upper limit of methanol proportion to 60%, reduce cycle variations and HC emissions, and improve the effective thermal efficiency. Under the diesel two-stage injection strategy, advancing the pilot injection timing delayed the heat release process, increased the peak value, and shortened the combustion duration, while advancing the main injection timing advanced the combustion process, increased the cylinder pressure and peak heat release, and resulted in increased NOx and soot emissions. Increasing the mass of diesel pre-injection led to earlier CA5 and combustion phases, transformed the heat release rate into a double-peak form, increased the cylinder pressure and brake thermal efficiency (BTE), and reduced HC and CO emissions.

The aforementioned work discussed the influence of various operating parameters on methanol-fueled engines. It can be seen that the direct injection strategy of high-reactivity fuels has a particularly significant impact on combustion and emissions. However, the influence of direct injection strategies on the detail combustion processes of the dual-fuel combustion process is still unclear. Therefore, this study adopted the optical engine platform to investigate the details of in-cylinder combustion processes fueled by a methanol/diesel dual fuel. It reveals in detail the underlying flame characteristics and flame development by combining high-speed photography and image processing techniques. This study will help to comprehensively understand the influence of the diesel injection timing on diesel/methanol dual-fuel combustion and provide a reference for regulating injection strategies and optimizing the combustion process.

2. Experimental Set-up and Procedure

2.1. Experimental Equipment

All of the experiments were conducted in a single-cylinder, four-stroke optical engine. Figure 1 shows the schematic diagram of the optical engine test platform, which consisted of seven parts: an optical engine, fuel supply system, cylinder pressure acquisition system, image acquisition system, intake heating system, lubricating oil circulation system, and water temperature control system.

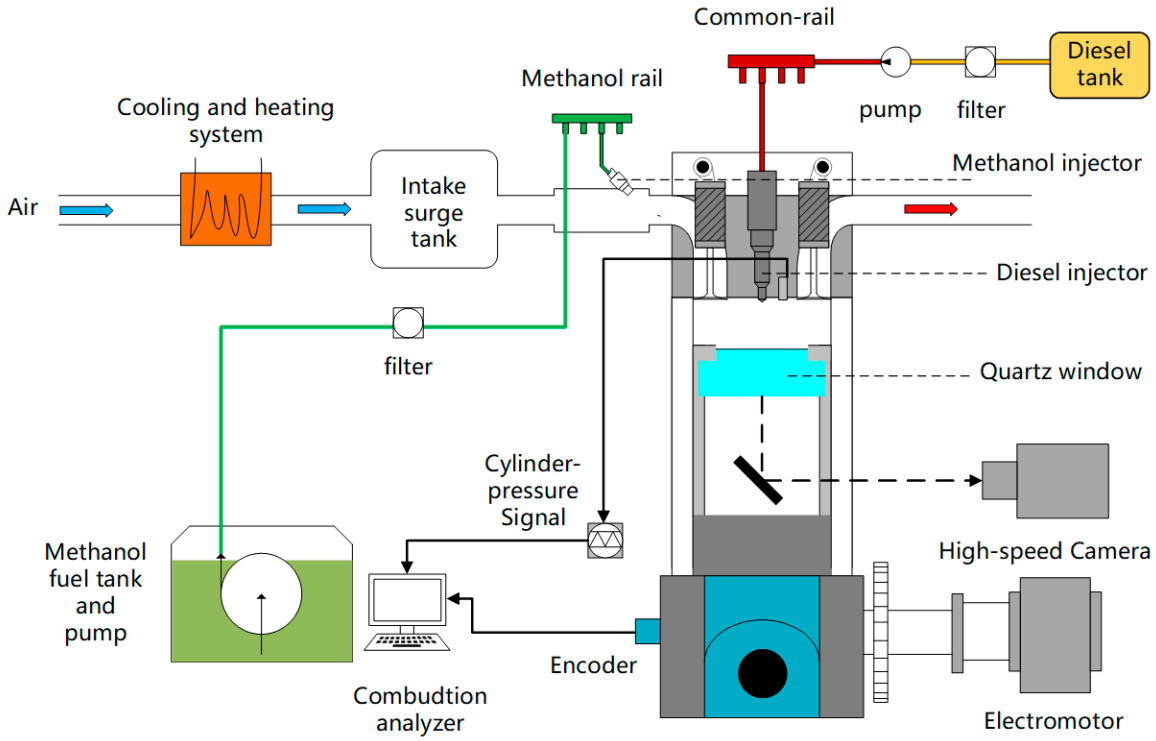

Figure 1. Schematic diagram of optical engine bench.

As shown in Figure 2, the combustion chamber and visualization area were designed so that the images of combustion inside the cylinder were captured by a high-speed camera through a quartz piston and a 45° angled mirror. Each test did not exceed 10 cycles because the optical components could not sustain large thermal and mechanical loads. The platform was equipped with an external lubricating oil circulation system and a high-pressure common rail system. Additionally, an independent port injection system was developed to achieve port injection of low-reactivity fuels, and its control program was integrated into the engine control unit (ECU). This allowed adjustments to the port injection pulse width and injection timing. Table 1 summarizes the parameters of the optical engine and fuel injection system.

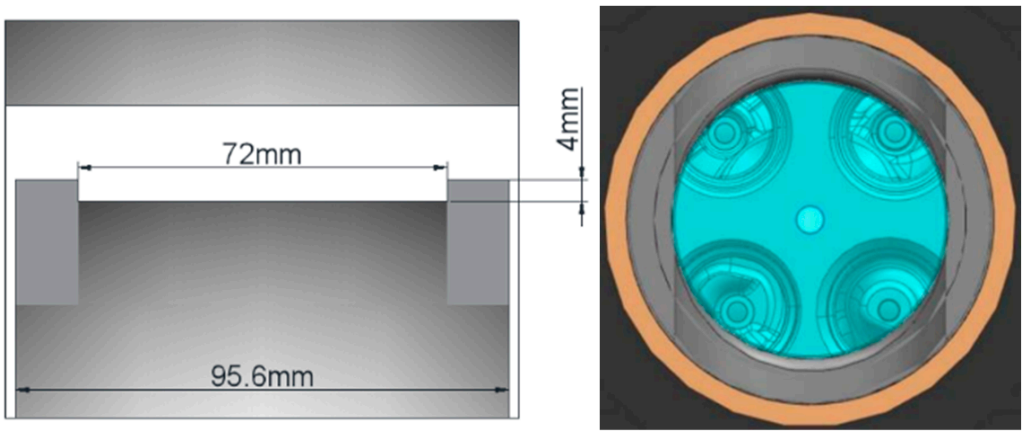

Figure 2. Diagram of the combustion chamber and the visualization area at the top dead center.

Table 1. The technical specifications of the engine and fuel injection system.

Item	Specification
Engine type	4 valve, single-cylinder, naturally aspirated
Cylinder diameter/stroke	96 mm/115 mm
Visible area diameter of piston	72 mm
Visible area height of piston	20 mm
Compression ratio	16.3
Common rail injector hole number	8
Injector hole diameter	0.147 mm
Spray angle	150°

To replicate the actual operating conditions of the engine more closely, an external water circulation heating system was equipped to heat the engine block and lubricating oil, ensuring that the test environment was close to the actual working state of the engine. The high-speed camera used in the experiment was a FASTCAM Mini AX200. The specific parameter settings are presented in Table 2.

Table 2. High-speed camera parameter settings.

Parameter	Value
Aperture	f/2.8
Shutter speed	1/20,000 s
Shooting speed	14,400 fps
Resolution	512 × 512

2.2. Test Fuels

Methanol (CH_3OH, up to 99.5% purity) and diesel (commercial ultra-low sulfur) were injected into the intake port and cylinder, respectively. Table 3 summarizes the properties of the methanol and diesel fuels.

Table 3. Properties of methanol and diesel fuels.

Properties	Methanol	Diesel
Formula	CH_3OH	$C_{8–25}$
Density/(kg/m^3)	798	840
Lower heating value (MJ/kg)	19.7	42.5
Volumetric energy density (GJ/m^3)	15.6	36.7
Stoichiometric A/F ratio	6.52	14.3
Auto-ignition temperature (K)	738	523–723
Minimum ignition energy (mJ)	0.215	0.8
Octane number (RON)	119	--
Flammability range (vol.%)	6.7~36	1.4~7.6
Content of O (wt%)	49.93	0

2.3. Experimental Procedure

First, the circulating water was heated to above 90 °C, and the lubricating oil was heated to 60~70 °C (with the oil pressure controlled at 0.2~0.3 bar). The engine block was heated to approximately 80 °C, and the cylinder pressure acquisition system, high-speed camera, high-pressure common rail system, and intake injection system were set to the ready-to-trigger state. A variable frequency motor was then used to control the engine up to 1200 r/min. Once the speed stabilized, the cylinder pressure acquisition program was initiated, and the ECU triggered the high-speed camera and injection system.

2.4. Image Processing Methods

To obtain more information about dual-fuel combustion, a set of MATLAB 2017a image processing codes was developed to extract the image's grayscale, flame area, and other relevant data. For better analysis of the combustion characteristics, the B and R channels were selected to separate the blue and yellow flames during image processing. Subsequently, appropriate thresholds were applied to convert the separated images into a black-and-white format, and the number of pixels occupied by the flame was counted to determine the flame area.

Due to the scattered distribution of flames in compression-ignition engines, this study employed the equivalent radius method to calculate the flame propagation speed using the following formula:

$$S_f = (dA/dt)/L_e \tag{1}$$

where S_f represents the flame speed, A is the projected area of the flame, t is the time interval between the images, and L_e represents the circumference of an equivalent circle [29] with the same area as the flame.

The brightness and color of the flame are strongly correlated with the combustion emission characteristics. It is generally believed that the bright yellow light observed during the combustion process is emitted by soot particles. Relevant studies have also shown that the development of yellow flames in the image represents the evolution of soot [30,31]. Therefore, the analysis of yellow flames can provide information on soot. In this study, the average signal intensity of yellow flames obtained using the average grayscale method was used to characterize the trend of the overall soot concentration changes within the cylinder.

3. Experimental Condition Setting

The experiment comprised two parts. The first part studied the impact of different methanol energy ratios while ensuring that the total energy of diesel and methanol in the cylinder remained constant and gradually increasing the methanol energy ratio. In the second part, when diesel was injected in multiple stages, the proportion of methanol energy was fixed, and the main injection time of diesel was varied to explore its impact. Due to the optical engine's limitations in withstanding high mechanical and thermal loads, the total fuel energy in the experiment was fixed at the equivalent diesel energy of 14 mg/cycle, with the direct injection pressure of diesel at 60 MPa. When diesel was injected in a single shot, the impact of different methanol energy ratios (30–80%) was explored at a diesel injection timing of −23 °CA ATDC. Meanwhile, when diesel was injected in multiple stages, the methanol energy ratio was fixed at 50%, with diesel pre-injection timings of −33 °CA ATDC and −58 °CA ATDC, and the main injection timing was varied from −11° to −23° to explore its influence. The schematic diagrams of fuel injection under the two operating conditions are shown in Figure 3.

In this article, the methanol energy ratio (MER) was calculated using the Equation (2), and the diesel pre-injection ratio (PIR) was calculated using the following formula:

$$MER = \frac{m_M \times LHV_M}{m_M \times LHV_M + m_D \times LHV_D} \tag{2}$$

$$PIR = \frac{m_{D-pre}}{m_{D-pre} + m_{D-main}} \tag{3}$$

In the above formulas, m_M and m_D represent the masses of injected methanol and diesel, respectively, in each cycle, LHV_M and LHV_D stand for the lower heating values of methanol and diesel, respectively, and m_{D-pre} and m_{D-main} represent the masses of the pre-injected diesel and main injected diesel, respectively.

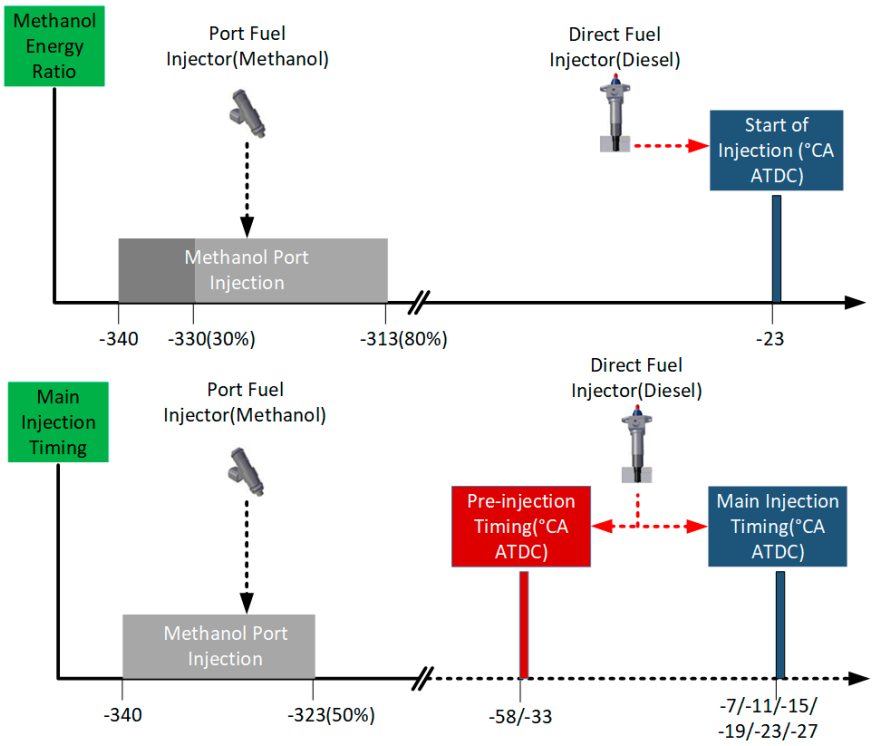

Figure 3. Schematic diagram of fuel injection strategy for different operating conditions.

4. Results and Discussion

Section 4.1 discusses the combustion characteristics and flame features under different methanol energy ratios, while Section 4.2 mainly focuses on the impact of varying the main diesel injection timing on the diesel/methanol dual-fuel combustion process with a fixed methanol energy ratio of 50%. In this article, the crank angles corresponding to the moments when the combustion heat release reached 5%, 10%, 50%, and 90% of the total heat release are defined as CA5, CA10, CA50, and CA90, respectively. The ignition delay period was defined as the time from the fuel injection timing to CA5, the combustion phase corresponded to the CA50 timing, and the combustion duration is represented by the period from CA10 to CA90.

4.1. Influence of Methanol Energy Ratios

This section changes the energy ratio between methanol and diesel based on the total fuel energy of 14 mg diesel equivalent for each cycle and discusses the combustion characteristics under different methanol energy ratios. The intake air temperature was 65 °C, the direct injection diesel pressure was 60 MPa, and the diesel injection timing was −23 °CA ATDC. Due to the minimum opening time limit of the methanol nozzle, the proportion of methanol energy injected into the intake port started at 0.3 and gradually increased to 0.8. The main operating conditions are shown in Table 4.

Figure 4 shows the cylinder pressure and heat release rate curves under different methanol energy ratios. It can be observed that at low methanol energy ratios, the peak cylinder pressure of the engine was relatively high. The peak cylinder pressure at a ratio of 0.4 did not differ much from that at a ratio of 0.3 and was even slightly higher. From the heat release rate curve, it can be seen that a higher peak heat release rate was observed at a ratio of 0.4. The main reason for this is that the increase in the methanol proportion led to a slight delay in the combustion heat release process, as reflected by the slightly late rise of the heat release rate in Figure 4, enabling the mixture to achieve a better combustion state and burn fully near the top dead center. As the methanol energy ratio further increased, the peak cylinder pressure decreased significantly, and there was a noticeable delay in the start of heat release. This was primarily due to the further increase in the proportion of

methanol with a high latent heat of vaporization, which significantly reduced the thermal condition in the cylinder due to fuel vaporization, as evidenced by the decrease in cylinder pressure near the top dead center. Secondly, the reduction in diesel injection quantity and the increase in the amount of low-reactivity methanol resulted in a decrease in the overall reactivity of the mixture, further causing delayed and deteriorated combustion conditions. When the methanol ratio reached 0.8, the peak value of the cylinder pressure curve was close to that of the motored cylinder pressure, and the heat release was slow, indicating a significant deterioration in the combustion condition. This suggests that at lower loads, the proportion of methanol energy should not be too high.

Table 4. Engine operation conditions for different methanol energy ratios.

Parameters	Value
Engine speed (r/min)	1200
Intake air temperature (°C)	65
Diesel mass (mg)	9.8, 8.4, 7, 5.6, 4.2, 2.8
Direct injection pressure (MPa)	60
Start of diesel injection (°CA ATDC)	−23
Start of methanol injection (°CA ATDC)	−340
Methanol injection pressure (bar)	4
Methanol energy ratio (%)	0.3, 0.4, 0.5, 0.6, 0.7, 0.8
Methanol injection mass (mg)	9.061, 12.081, 15.102, 18.122, 21.142, 24.16

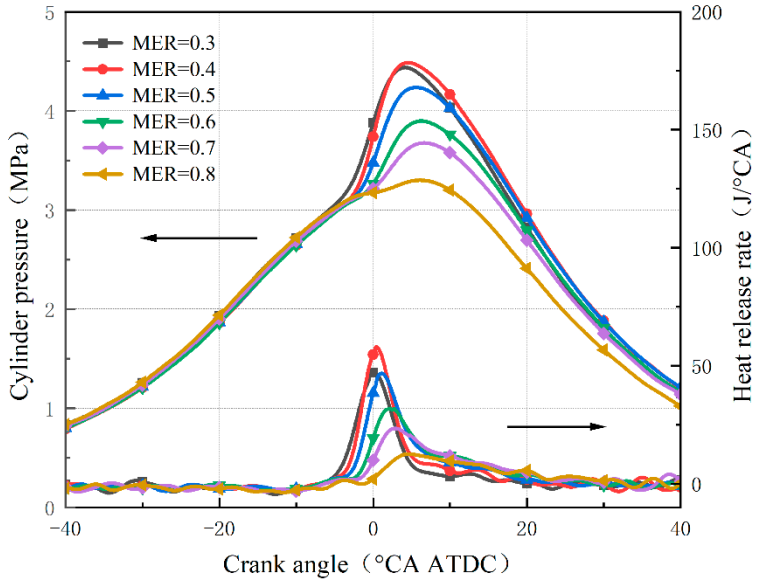

Figure 4. Cylinder pressure and heat release rate curves under different methanol energy ratios.

Figure 5 demonstrates the changes in the combustion characteristic parameters. Specifically, the ignition delay increased and combustion phase CA50 delayed correspondingly with the increase in the methanol proportion. This was primarily due to the reduction in the overall reactivity of the mixture and the reduction in the cylinder temperature. The combustion duration was shortened at a methanol ratio of 0.4, while there was little difference at other ratios, which corresponded to the concentrated heat release process near the top dead center under this ratio.

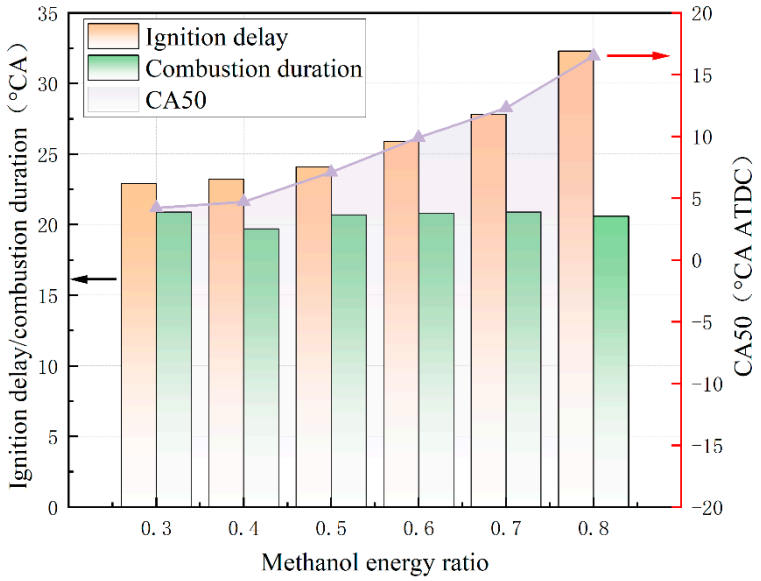

Figure 5. The variation in the ignition delay, combustion duration, and CA50 under different methanol energy ratios.

Figure 6 illustrates the trend of indicated thermal efficiency with the increase in methanol energy, which rose first and then decreased. Notably, a severely low thermal efficiency was observed at a methanol ratio of 0.8. When the methanol energy proportion was relatively small, the higher peak cylinder pressure enabled the engine to produce more work, and the combustion efficiency was also relatively high, resulting in a higher indicated thermal efficiency for the engine. However, when methanol accounted for half of the total energy, the reduction in the active and thermal conditions within the cylinder led to a slow and delayed heat release process, resulting in incomplete fuel combustion within the cylinder and a significant reduction in the engine's thermal efficiency.

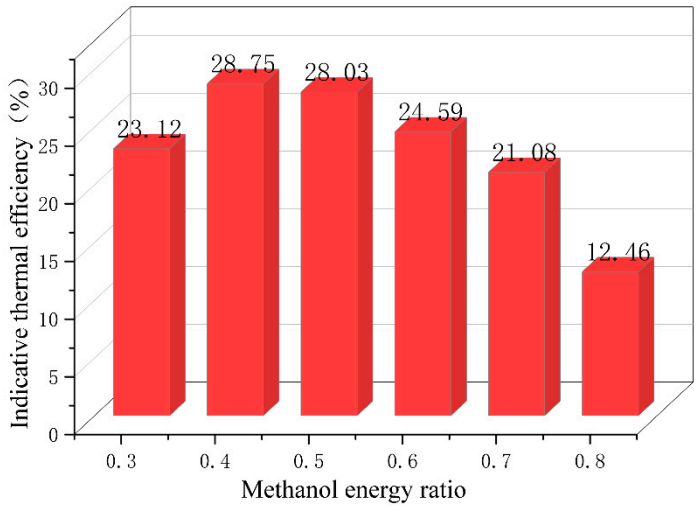

Figure 6. The indicative thermal efficiency (ITE) under different methanol energy ratios.

Figure 7 displays the direct chemiluminescence images of flames under different methanol ratios. To better visualize the details of the images, brightness enhancement processing was applied to all of the images. It can be observed that with the increase in the methanol ratio, the ignition timing generally exhibited a delayed trend. At a low methanol premixed ratio of 0.3, both blue and yellow flames appeared simultaneously near the wall downstream of the diesel spray at a −5° crank angle. Subsequently, the flame gradually propagated toward the center of the combustion chamber, exhibiting a

distinct spray-guided combustion pattern. This was due to the high proportion of diesel in the total fuel energy at this point. After a short ignition delay, the diesel failed to mix uniformly with the cylinder charge, resulting in some diesel acting as an ignition enhancer to promote premixed combustion of the mixture, while the rest of the diesel underwent incomplete combustion due to a fuel-rich and oxygen-poor state, producing a bright yellow flame. When the methanol energy ratio reached 0.4, the initial flame in the viewport was primarily blue and covered a larger area. The reduced mass of diesel fuel and the extended gas mixing time resulted in a more homogeneous mixture such that the bright yellow flame was barely visible in the initial field of view. The larger blue flame area during the initial combustion stage was mainly due to the longer mixing time between diesel and methanol, as well as the increase in the methanol equivalence ratio, which promoted more premixed gas reaching the reaction conditions and combusting simultaneously. As the methanol ratio was further increased, especially when it exceeded 0.5, the timing of the first flame appearance was significantly delayed, and the flame coverage area was notably reduced. The yellow flame was mainly concentrated in the central region, and a large area between the wall and the center position remained flame-free. This was primarily due to the decrease in the overall reactivity of the fuel in the cylinder and the weakening of the diesel ignition ability. The blue flame was concentrated near the cylinder wall, while the yellow flame was mostly in the form of scattered autoignition sites due to the reduction in the total amount of diesel fuel, resulting in smaller areas reaching flammable conditions.

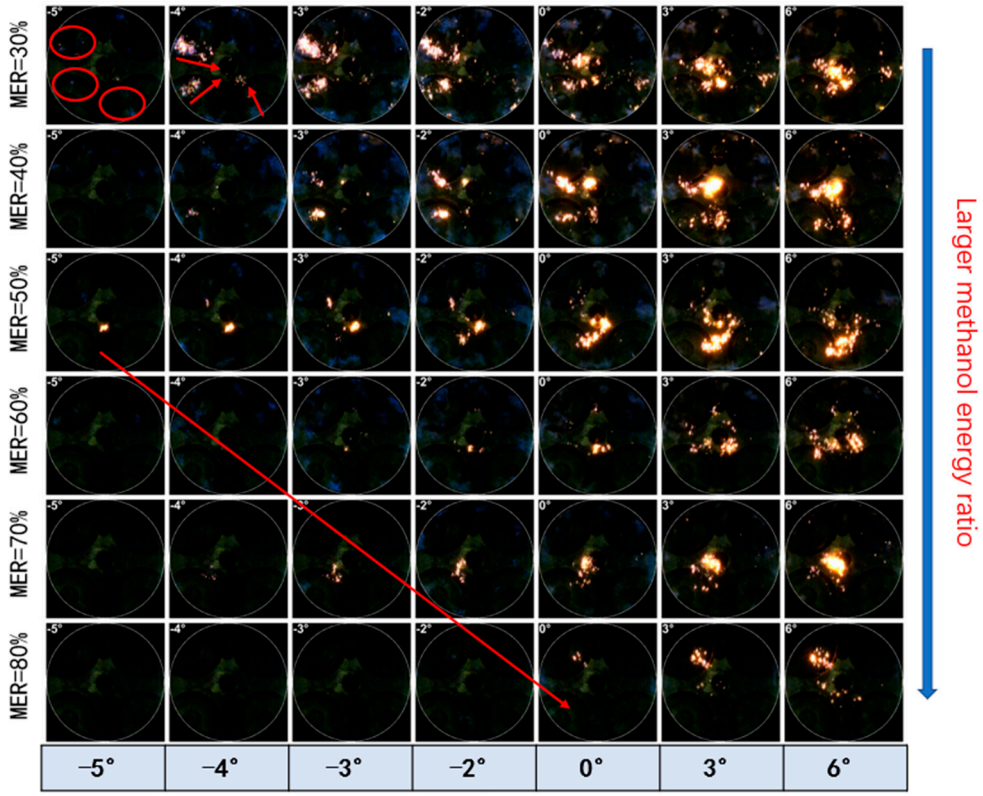

Figure 7. Self-luminous images under various methanol energy ratios.

Figure 8a–c depicts the yellow, blue, and total flame areas, respectively. As the methanol substitution ratio increased, the peak areas of both the yellow and blue flames exhibited a trend of first increasing and then decreasing. Additionally, since the premixed flame of diesel/methanol dominated the early stage, the crank angle of the blue flame area peak occurred earlier than that of the yellow flame. When the ratio was below 0.5, due to the earlier injection timing and the involvement of a large amount of diesel in the premixed combustion of methanol, the peak area of the blue flame was higher than that of the yellow flame. However, as the methanol ratio further increased, the ignition ability of

diesel decreased significantly, leading to a reduction in the amount of ignited methanol and a decrease in the blue flame area, which could be even lower than the yellow flame area. From the perspective of the total flame area, a double-peak phenomenon was observed in most cases. The peak before the top dead center was dominated by the premixed blue flame. Subsequently, the blue flame area decreased while the yellow flame area increased, and the interaction between the two resulted in the second peak after the top dead center.

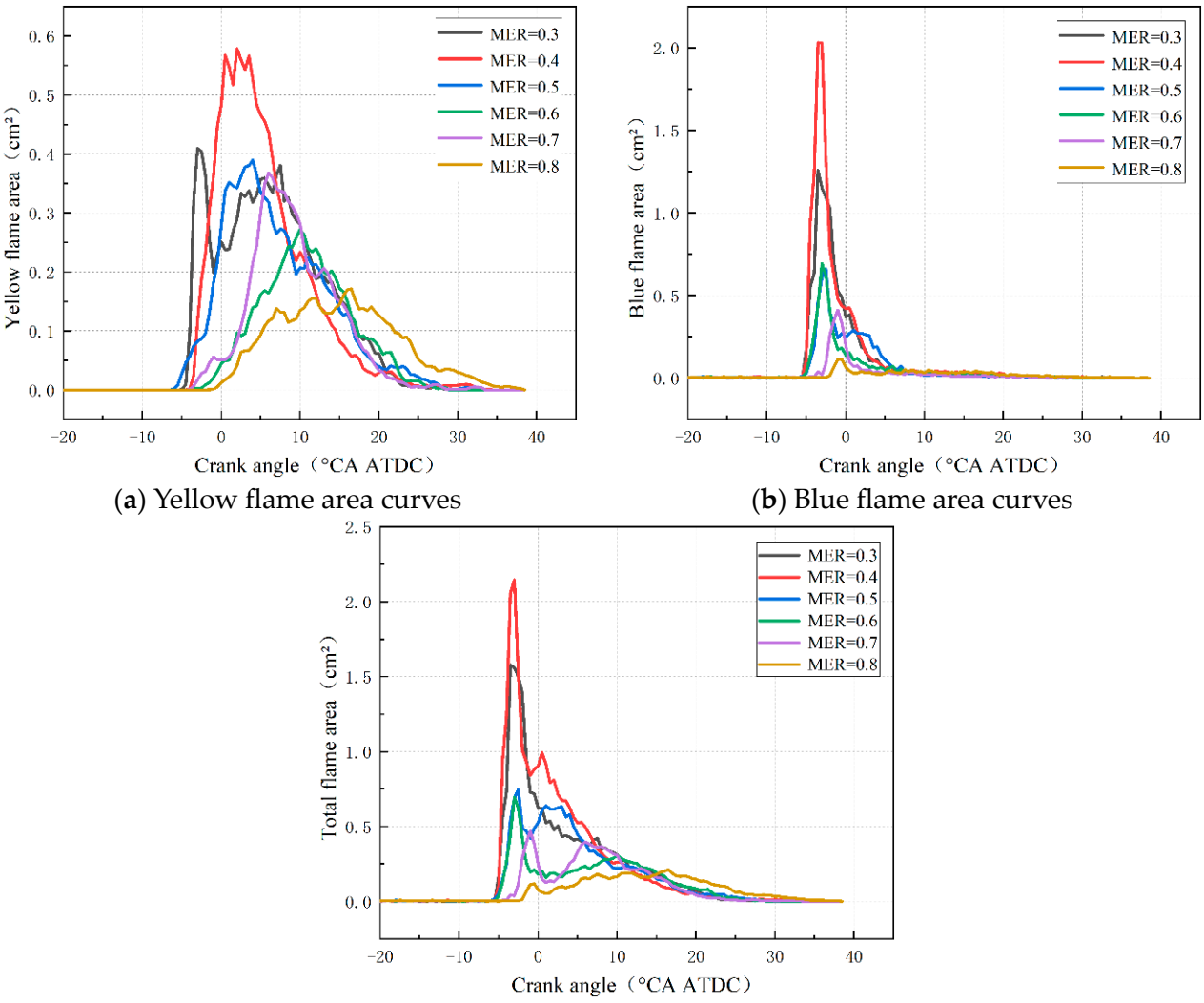

Figure 8. Yellow, blue, and total flame areas under different methanol energy ratios.

In Figure 9, under various energy ratios, the peak velocity of the blue flame is significantly higher than that of the yellow flame, demonstrating the significant advantage of the premixed combustion mode in terms of combustion speed. At the same time, as the methanol energy ratio increased, the overall combustion speed first increased and then decreased. When diesel dominated the total energy, the engine exhibited a higher overall combustion speed. However, when diesel did not occupy a primary position in the energy ratio, the reactivity and thermal atmosphere of the mixture in the cylinder decreased, resulting in poorer overall combustion and a significant reduction in flame speed. Therefore, under low loads, the methanol energy ratio should not exceed 0.5.

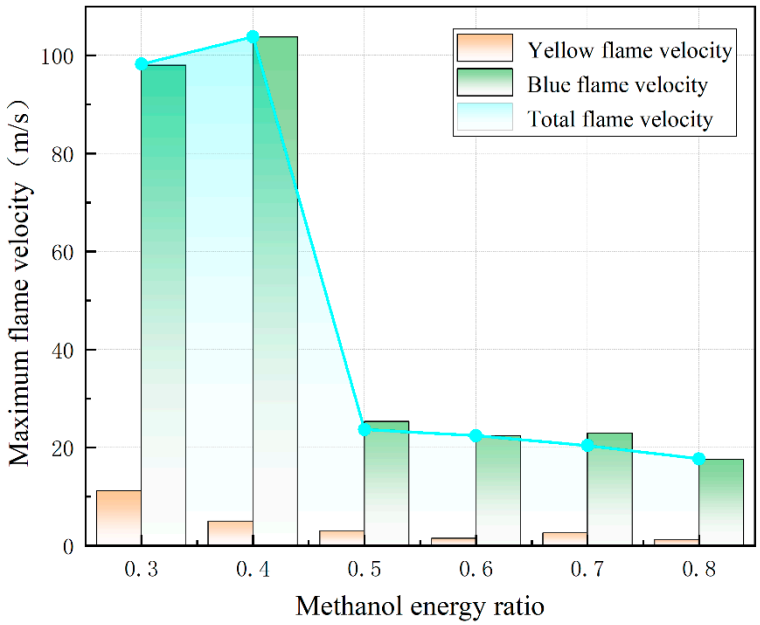

Figure 9. Maximum flame velocity under different methanol energy ratios.

In Figure 10, the signal intensity of the yellow flame represents the soot concentration during the combustion process, and its peak generally followed a trend of first increasing and then decreasing. This was because of the fact that the overall combustion was promoted with a methanol ratio of 0.4, resulting in higher combustion temperatures within the cylinder and the generation of more soot. Additionally, the shortened ignition delay period led to insufficient mixing of diesel and air, further increasing the factors that contribute to soot formation. However, at higher methanol ratios, the reduction in diesel mass and combustion temperature promoted a decrease in soot generation. When observing the timing of the peak brightness of the yellow flame, it can be seen that it generally occurred later, mainly due to the decrease in the amount of directly injected fuel, which led to a reduction in the fuel concentration gradient within the cylinder. This delayed the diesel diffusion combustion process, and during the expansion stroke, the flame propagation speed decreased, resulting in slower combustion.

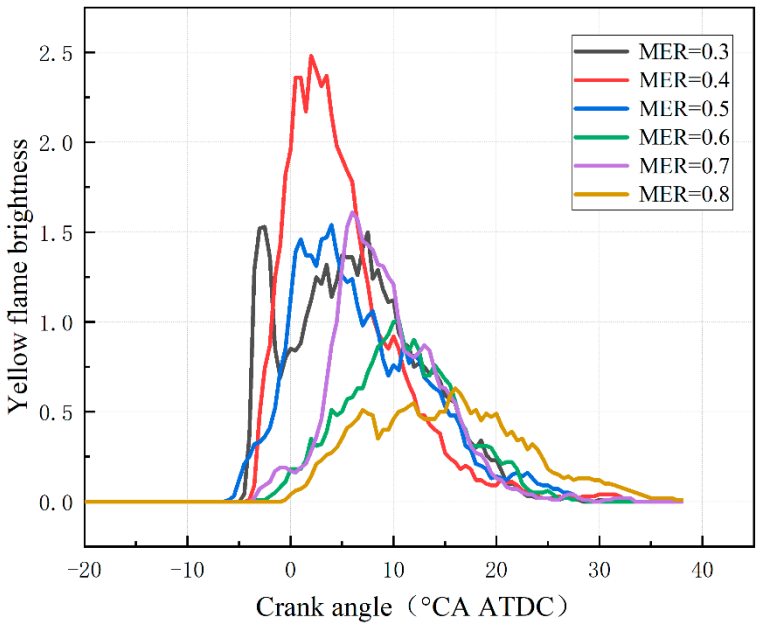

Figure 10. Yellow flame brightness under different methanol energy ratios.

4.2. Influence of Diesel Split Injection Strategies

Split injection of diesel can regulate the stratification of the air-fuel mixture, making it an effective means to control and improve combustion. The effects of different diesel split injection strategies are investigated further for the unsatisfactory combustion conditions observed at a relatively high methanol energy ratio of 50% in Section 4.1. In this section, the proportion of diesel pre-injection was fixed at 50%, and two pre-injection timings of −58° and −33° were selected for exploration. The diesel main injection timings were set to −11°, −15°, −19°, and −23°, respectively. The main operating conditions are summarized in Table 5 below.

Table 5. Engine operation conditions for different diesel main injection timings.

Parameters	Value
Engine speed (r/min)	1200
Intake air temperature (°C)	65
Direct injection pressure (MPa)	60
Total diesel mass (mg)	7
Diesel pre-injection timing (°CA ATDC)	−58, −33
Diesel main injection timing (°CA ATDC)	−7, −11, −15, −19, −23, −27
Diesel pre-injection ratio (%)	50
Methanol injection mass (mg)/energy ratio	15.10/0.5
Start of methanol injection (°CA ATDC)	−340

Figure 11 shows the cylinder pressure and heat release curves for different main injection timings under two pre-injection timings. The heat release synchronously varied with the advancement of the main injection timing, reflecting the effective control of the main injection on combustion initiation. As shown in Figure 11a, when the PIT was set to −58°, the cylinder pressure peaks and peak heat release rates were generally lower compared with the PIT = −33° condition, and there was a longer period of low heat release rates during the later stages of combustion. This is because an earlier diesel pre-injection timing significantly increases the mixing time between diesel and methanol-air, reducing the degree of fuel stratification and resulting in the formation of more lean mixtures within the combustion chamber. This lowers the local reactivity, and partially unreacted fuel undergoes slow oxidation and combustion during the later stages of combustion. From the cylinder pressure curves, it can be seen that as the main injection timing was advanced, the cylinder pressure peak continuously increased but slightly decreased at a main injection timing of −27°. This is because the mixture became more homogeneous at this point, and the in-cylinder atmosphere had a significant impact on combustion. As can be observed in Figure 11b, when the pre-injection timing (PIT) was set at −33°, the cylinder pressure peaks generally remained at a relatively high level. At a main injection timing of −7°, the pressure peak generated by combustion was lower than the compression pressure at the top dead center (TDC). As the main injection timing was advanced, the cylinder pressure peaks increased continuously, and their phase shifted significantly earlier, with all main injection timings resulting in cylinder pressure peaks above 4 MPa. In terms of the heat release rate curves, a main injection timing of −7° resulted in a flatter heat release curve with a lower peak heat release rate and a longer duration of the heat release process. This was due to the combustion process occurring far from the TDC, leading to delayed auto-ignition events and slower flame propagation during the expansion stroke. When the main injection timing was advanced, the difference in the peak heat release rates was small, but their phases continued to advance, resulting in an overall "high and narrow" characteristic of the heat release curve. Overall, when the PIT was set to −33°, there was a larger variation in cylinder pressure peaks, primarily due to the strong control of the main injection timing on the combustion phase.

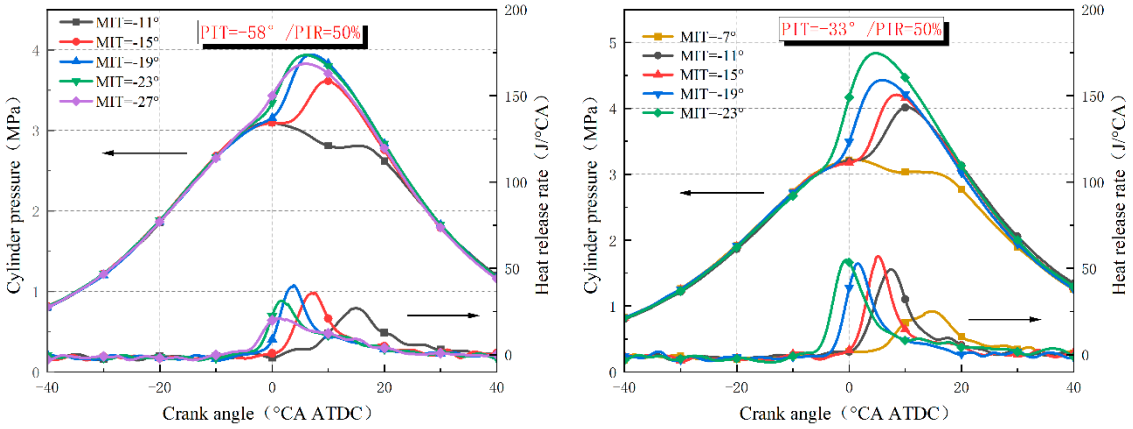

(**a**) PIT = −58° (**b**) PIT = −33°

Figure 11. Cylinder pressure and heat release rate at each main injection timing when PIT = −58° and −33°.

Figure 12a,b presents the ignition delay, combustion phase, and combustion duration at various main injection timings. Overall, a later pre-injection timing (PIT = −33°) resulted in a shorter ignition delay. This is because the stratification effects of the mixture caused by different pre-injection timings differed, with a later pre-injection timing creating local rich combustion zones and favorable combustion conditions for rapid ignition after the main injection. As the main injection timing was advanced, the changes in ignition delay under both pre-injection timings showed similar patterns, initially decreasing and then increasing. However, the changes in the combustion phase under the two pre-injection timings differed. With a pre-injection timing of −33°, the combustion phase advanced with the advancement of the main injection timing. In contrast, with a pre-injection timing of −58°, the combustion phase initially advanced with the advancement of the main injection timing but was then slightly delayed due to the deteriorating thermal condition within the cylinder at the main injection timing. This indicates that the main injection timing can significantly regulate both the start of combustion and the combustion phase, while the combustion phase under an earlier pre-injection timing is still largely influenced by the in-cylinder environment when the main injection happens.

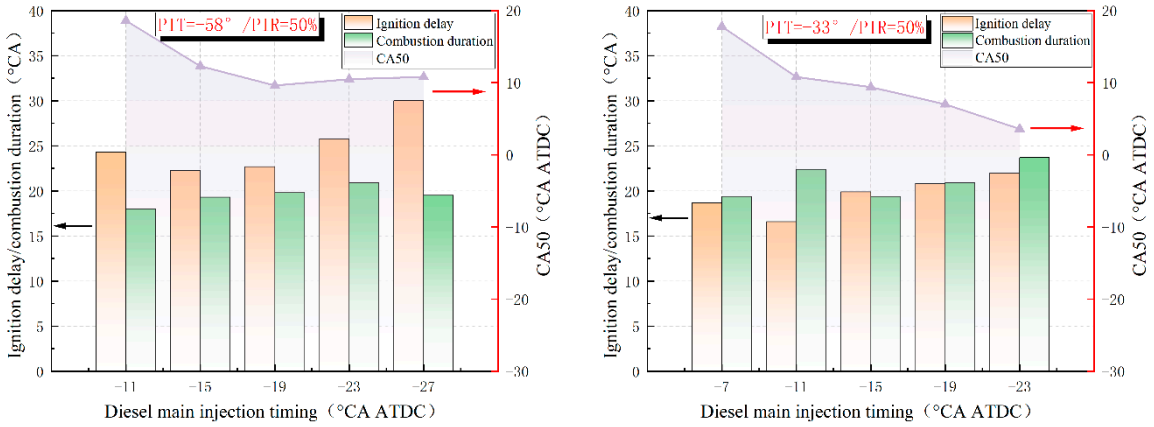

(**a**) PIT = −58° (**b**) PIT = −33°

Figure 12. The variation in ignition delay, combustion duration, and CA50 at each main injection timing when PIT = −58 ° and −33°.

As shown in Figure 13, the indicated thermal efficiency under PIT = −33° was higher overall than that under PIT = −58°. This is because under a later pre-injection timing, the combinations of various main injection timings could generate more combustion pressure

and a more optimized CA50. Meanwhile, under both pre-injection timings, the indicated thermal efficiency exhibited a similar pattern of change, with the highest indicated thermal efficiency achieved at intermediate main injection timings. Main injection timings which are too early or too late will lead to a decrease in the indicated thermal efficiency. This is because an early main injection timing can increase the negative compression work and result in slow combustion, while a late main injection timing can occur during the piston's downward stroke, far from the top dead center, leading to lower work efficiency and increased heat loss, both of which contribute to a decrease in the indicated thermal efficiency.

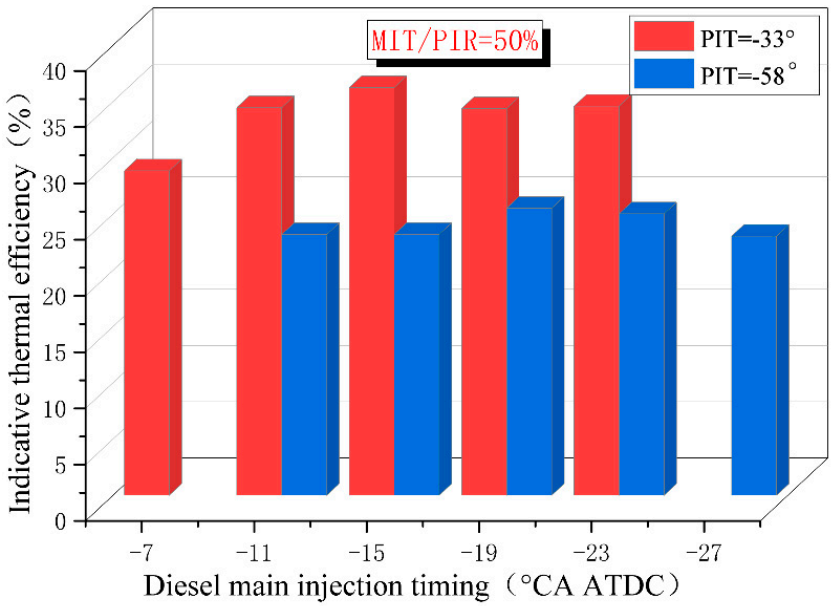

Figure 13. The ITE at each main injection timing when PIT = −33° and −58°.

Figure 14 presents a sequence of combustion images at PIT = −58°. As the main injection timing was advanced, the emergence of ignition points in the images occurred earlier overall. Due to the deterioration of the thermal condition where the main injection diesel was located and the prolongation of the ignition delay, the time interval between the appearance of the blue flame and yellow flame kernel was shortened. At a main injection timing of −11°, the blue flame appeared 2° after the auto-ignition kernel formation. However, at a main injection timing of −27°, the blue flame appeared even earlier than the yellow flame kernel. In the subsequent flame development process, as the main injection timing increased from −11° to −19°, the blue flame covered a larger area and extended further toward the center of the combustion chamber due to the better in-cylinder thermal condition during the initial combustion process, which was closer to the top dead center. As the main injection timing continued to advance, the yellow flame and blue flame became more dispersed, and the coverage area decreased. At a main injection timing of −27°, the yellow flame was scattered around the chamber, and hardly any continuous flame could be observed, indicating that the fuel-air mixture was premixed too much and resulting in a slow and unstable low-temperature-dominated combustion process. Overall, when the pre-injection timing was earlier (PIT = −58°), the methanol contained within the blue flame was primarily ignited by compression autoignition during the early stages of combustion. Given the poor in-cylinder condition formed before the main injection, it is not advisable to adopt an excessively early diesel main injection timing.

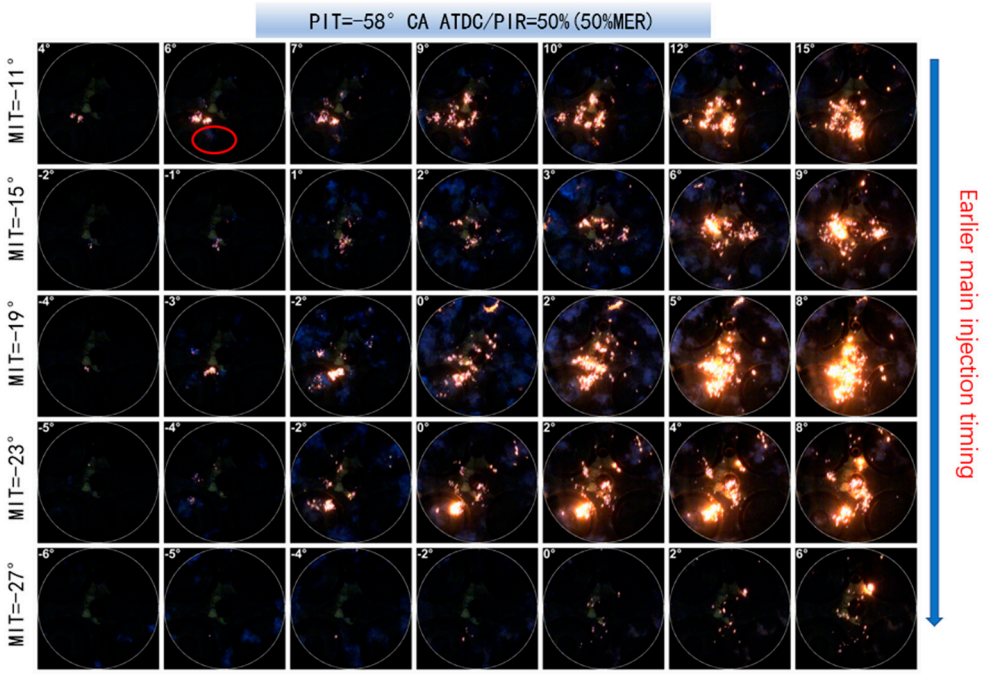

Figure 14. Self-luminous images at each main injection timing when PIT = −58°.

Figure 15 shows a sequence of combustion images at different main injection timings at PIT = −33°. Overall, the combustion process was more intense, with a higher flame brightness and a more concentrative flame distribution compared with those at PIT = −58°, reflecting the overall regulatory effect of the pre-injection timing on combustion. Due to the shorter ignition delay, the flame at each main injection timing exhibited a spray jet-like distribution. It can be observed that at a main injection timing of −7°, partial ignition sites appeared before the end of the main injection fuel injection. Upon completion of the injection, the flame kernel rapidly developed into a long, sheet-like flame along the fuel spray direction, emitting a bright incandescent light. Subsequently, new ignition points were formed in other fuel spray directions, and the flame developed along the fuel spray direction, expanding toward the surrounding areas and covering most of the combustion chamber. At a main injection timing of −11°, the flame development pattern was similar to that at −7°, except that a small amount of blue flame was observed at the edges of the yellow flame. This was due to the strong soot luminescence in the fuel spray area covering the blue flame produced by the premixed methanol/diesel combustion. At a main injection timing of −15°, the ignition points were more concentrated and closer to the edge of the viewport. Subsequently, the ignition points developed into sheet-like yellow flames which expanded radially outward. At the same time, large patches of light blue flame appeared in the surrounding areas, expanding and merging until filling the combustion chamber. At a main injection timing of −19°, the initial ignition characteristics were similar to those at −15°, but the yellow flame was mainly concentrated in the center of the combustion chamber, and the blue flame almost filled the peripheral areas. At this point, a large amount of premixed diesel and methanol was ignited. At a main injection timing of −23°, more dispersed yellow ignition points were formed at the initial stage of ignition, accompanied by a large area of blue flame (mainly cold flame) along the fuel spray direction. In the later stages of development, a large amount of blue flame mixed with yellow ignition sites appeared in the peripheral areas of the central region, while the yellow flame in the central region continued to merge and expand. Overall, the methanol contained within the blue flame was mainly ignited by the propagating flame during the middle stage of combustion. Starting from a main injection timing of −11°, as the main injection timing was advanced, the characteristics of premixed combustion became more pronounced, with an increase in the coverage area of the blue flame and a decrease in the area of the yellow flame.

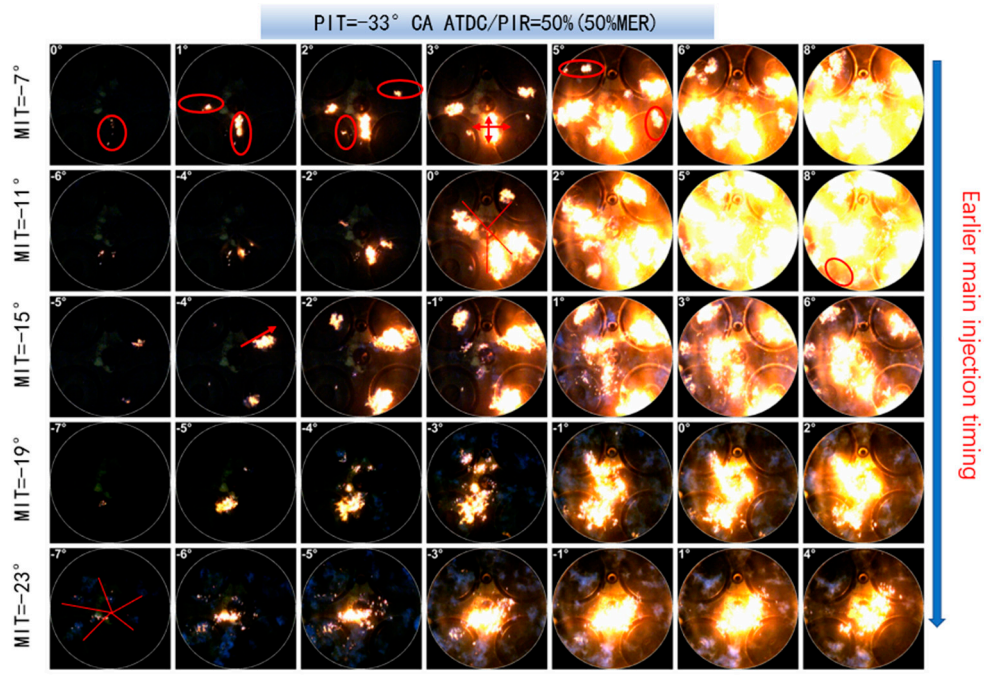

Figure 15. Self-luminous images at each main injection timing when PIT = −33°.

From the flame area graphs (Figures 16 and 17), it can be observed that at PIT = −33°, the overall area of the yellow flame was higher while the area of the blue flame was lower, and the peak phases of both flame areas occurred earlier than under the PIT = −58° condition. This is because with a later pre-injection timing, the thermal condition before the main injection was better, and the fuel stratification was higher. The main injection ignited quickly, and intense combustion occurred in some high-concentration, high-reactivity regions, producing bright yellow flames and a large amount of soot. Some of the soot emitted intense light, possibly obscuring the blue flame and leading to a smaller recognized area for the blue flame. (Under main injection timings of −7° and −11°, the blue flame was almost completely covered by the soot emissions.) At PIT = −58°, the peak areas of both the yellow and blue flames showed a consistent trend, initially increasing and then decreasing as the main injection timing was advanced. Overall, the peak timings of the yellow and blue flame areas were closer at each main injection timing (compared with PIT = −33°). This is because under the pre-injection timing of −58°, the mixture was in a more homogeneous state, with the main diesel and methanol participating in premixed compression ignition combustion while less participated in the subsequent diffusive combustion. When observing the flame areas at PIT = −33°, it can be seen that as the main injection timing was advanced, the peak area of the yellow flame decreased, while the peak area of the blue flame increased, displaying a complementary relationship between the two. This was due to the extension of the ignition delay period, resulting in a more homogeneous mixture and the ignition of more premixed diesel/methanol. Additionally, under later main injection timings, the combustion emitted intense incandescent light, and some of the blue flames may have been obscured and unobservable. Figure 18a,b shows the maximum flame speeds at PIT = −58° and PIT = −33°, respectively. It can be seen that under each main injection timing, the maximum yellow flame speed was generally higher at PIT = −33°, while the maximum blue flame speed was lower (except at a main injection timing of −23°). This is because at PIT = −33°, the reactivity and thermal atmosphere before ignition were better, allowing the diesel diffusion flame to propagate rapidly after the main injection. However, at PIT = −58°, the diesel and the premixed gas were uniformly mixed, resulting in the formation of multiple zones of simultaneous spontaneous ignition of the blue flame during ignition. But at a main injection timing of −23°, many regions of the mixture were too lean to combust due to excessive dilution.

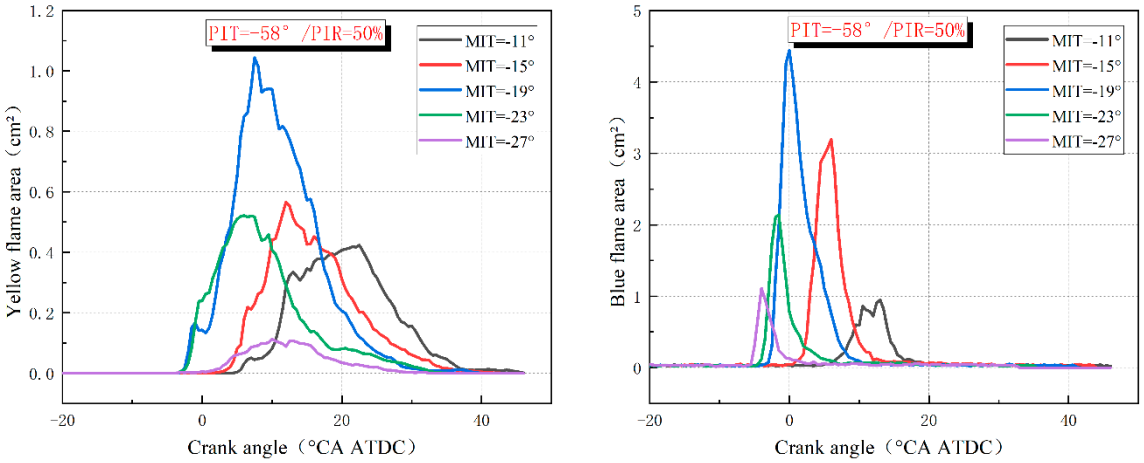

(**a**) Yellow flame area curves (**b**) Blue flame area curves

Figure 16. Yellow and blue flame areas at each main injection timing when PIT = −58°.

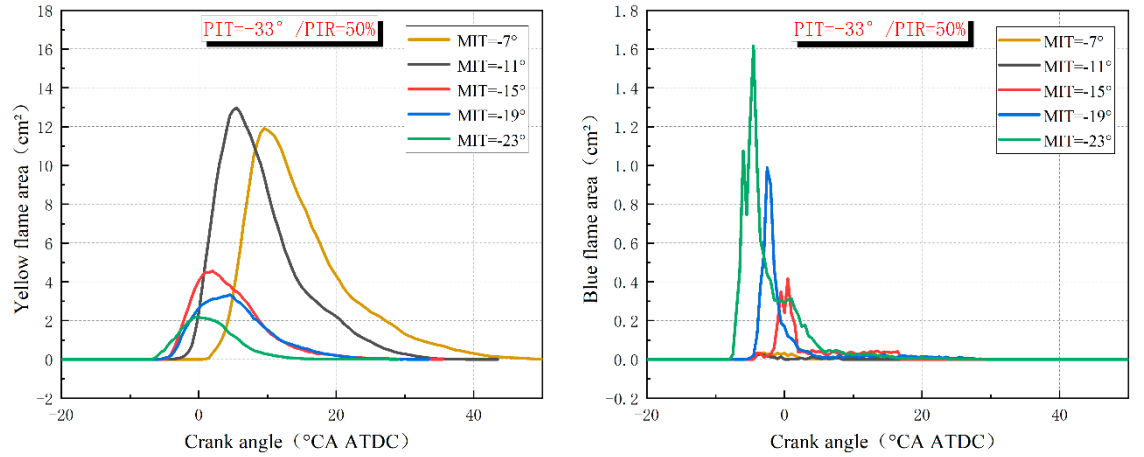

(**a**) Yellow flame area curves (**b**) Blue flame area curves

Figure 17. Yellow and blue flame areas at each main injection timing when PIT = −33°.

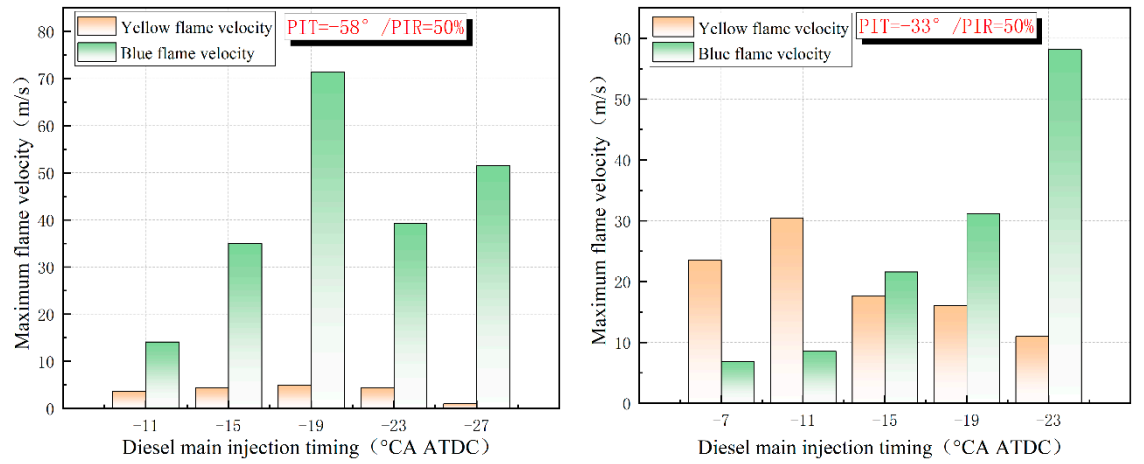

(**a**) PIT = −58° (**b**) PIT = −33°

Figure 18. Maximum flame velocity at each main injection timing when PIT = −58° and −33°.

Figure 19a,b shows the changes in the yellow flame intensity under PIT = −33° and PIT = −58°, respectively. It is evident that the yellow flame intensity was significantly

higher at PIT = −33° and differed by orders of magnitude compared with that at PIT = −58°. This is because at PIT = −58°, the yellow flame intensity was extremely low at a main injection timing of −27°, as the main injection occurred in colder cylinder conditions with unstable combustion. The yellow flame mainly appeared as fine yellow flame kernels. In contrast, at PIT = −33°, the rapid ignition after the main injection generated a large amount of soot. The yellow flame intensities at main injection timings of −7° and −11° were significantly higher than those at other earlier injection timings. At these timings, the ignition points already formed in the cylinder during the injection of the main fuel, resulting in the main fuel not having enough time to mix with the air and undergoing intense diffusive combustion. Therefore, under later pre-injection timings, the main injection timing should not be too close to the top dead center.

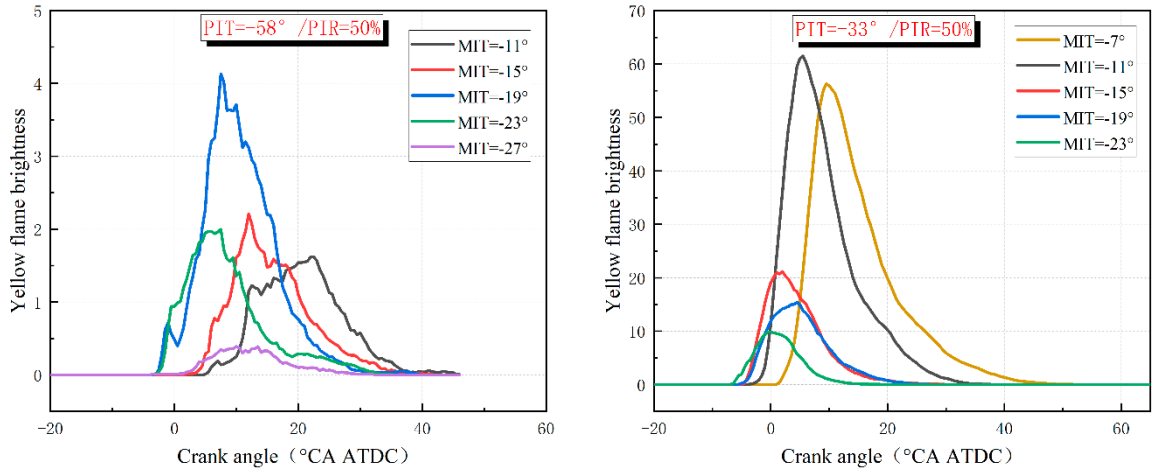

(**a**) PIT = −58° (**b**) PIT = −33°

Figure 19. Yellow flame brightness at each main injection timing when PIT = −58° and −33°.

5. Conclusions

In this study, the detailed combustion characteristics and underlying combustion mechanism in ICE fueled by methanol/diesel dual fuel was investigated in an optical single-cylinder diesel engine. The conclusions are as follows:

- Considering the low reactivity of methanol and its high latent heat of evaporation, its combustion relies on the in-cylinder atmosphere created by diesel fuel. When engaging in dual-fuel combustion, it is vital to consider the overall reactivity of the fuel. Controlling the upper limit of the methanol ratio is important to avoid a significant decrease in the flame area, which can lead to a notable decline in the peak cylinder pressure and heat release rate, ultimately resulting in deterioration of the combustion conditions.
- Analysis of combustion images indicates that the premixed blue flame tended to be concentrated near the walls, while the yellow flame resulting from diesel combustion tended to concentrate toward the center. The flame had a spray jet-like shape, and during the middle stages of diffusion combustion, the methanol within the blue flame was primarily ignited by the yellow flame.
- Through optimization of the diesel fuel injection strategy, such as the implementation of a single injection with precise advance injection timing or split injection with later pre-injection moments, it is feasible to significantly enhance the specific mixture stratification combustion and atmosphere in the cylinder. This results in the improved overall combustion of methanol/diesel dual fuel and the generation of intense incandescence. Consequently, there is a notable increase in the cylinder pressure, peak heat release rate, and indicated thermal efficiency.

Author Contributions: Methodology, J.W.; Software, H.Z.; Investigation, Z.Z. and W.O.; Writing—original draft, Z.Z.; Writing—review & editing, H.Z., X.W. and Z.W.; Supervision, Z.W. All authors have read and agreed to the published version of the manuscript.

Funding: The paper was supported by National Key Laboratory of Marine Engine Science and Technology. The authors also acknowledge the project of Combustion and Emission Control Technologies Research for Ammonia-fueled Marine Engines based on the Diesel Cycle.

Data Availability Statement: The original contributions presented in the study are included in the article, further inquiries can be directed to the corresponding author.

Conflicts of Interest: The authors declare that they have no known competing financial interests or personal relationships that could have appeared to influence the work reported in this paper.

Nomenclature

CI	Compression ignition
BTE	Brake thermal efficiency
ECU	Engine control unit
MER	Methanol energy ratio
PIR	Pre-injection ratio
ITE	Indicative thermal efficiency
PIT	Pre-injection timing
TDC	Top dead center
CA10	Crank angle with fuel mass fraction burned at 10%
CA50	Crank angle with fuel mass fraction burned at 50%
CA90	Crank angle with fuel mass fraction burned at 90%
ICE	Internal combustion engine

References

1. Reitz, R.D. Directions in internal combustion engine research. *Combust. Flame* **2013**, *160*, 1–8. [CrossRef]
2. Musculus, M.P.B.; Miles, P.C.; Pickett, L.M. Conceptual models for partially premixed low-temperature diesel combustion. *Prog. Energ. Combust.* **2013**, *39*, 246–283. [CrossRef]
3. Senecal, P.K.; Leach, F. Diversity in transportation: Why a mix of propulsion technologies is the way forward for the future fleet. *Results Eng.* **2019**, *4*, 100060. [CrossRef]
4. Khandal, S.V.; Banapurmath, N.R.; Gaitonde, V.N.; Hiremath, S.S. Paradigm shift from mechanical direct injection diesel engines to advanced injection strategies of diesel homogeneous charge compression ignition (HCCI) engines—A comprehensive review. *Renew. Sustain. Energy Rev.* **2017**, *70*, 369–384. [CrossRef]
5. Yu, S.; Zheng, S.; Li, X. The achievement of the carbon emissions peak in China: The role of energy consumption structure optimization. *Energ. Econ.* **2018**, *74*, 693–707. [CrossRef]
6. Saxena, M.R.; Maurya, R.K.; Mishra, P. Assessment of performance, combustion and emissions characteristics of methanol-diesel dual-fuel compression ignition engine: A review. *J. Traffic Transp. Eng. (Engl. Ed.)* **2021**, *8*, 638–680. [CrossRef]
7. Li, C.; Bai, H.; Lu, Y.; Bian, J.; Dong, Y.; Xu, H. Life-cycle assessment for coal-based methanol production in China. *J. Clean. Prod.* **2018**, *188*, 1004–1017. [CrossRef]
8. Börjesson, P.; Tufvesson, L.M. Agricultural crop-based biofuels—Resource efficiency and environmental performance including direct land use changes. *J. Clean. Prod.* **2011**, *19*, 108–120. [CrossRef]
9. Brynolf, S.; Fridell, E.; Andersson, K. Environmental assessment of marine fuels: Liquefied natural gas, liquefied biogas, methanol and bio-methanol. *J. Clean. Prod.* **2014**, *74*, 86–95. [CrossRef]
10. Bayraktar, H. An experimental study on the performance parameters of an experimental CI engine fueled with diesel–methanol–dodecanol blends. *Fuel* **2008**, *87*, 158–164. [CrossRef]
11. Datta, A.; Mandal, B.K. Impact of alcohol addition to diesel on the performance combustion and emissions of a compression ignition engine. *Appl. Therm. Eng.* **2016**, *98*, 670–682. [CrossRef]
12. Huang, Z.; Lu, H.; Jiang, D.; Zeng, K.; Liu, B.; Zhang, J.; Wang, X. Combustion behaviors of a compression-ignition engine fuelled with diesel/methanol blends under various fuel delivery advance angles. *Bioresour. Technol.* **2004**, *95*, 331–341. [CrossRef] [PubMed]
13. Huang, Z.H.; Lu, H.B.; Jiang, D.M.; Zeng, K.; Liu, B.; Zhang, J.Q.; Wang, X.B. Combustion characteristics and heat release analysis of a compression ignition engine operating on a diesel/methanol blend. *Proc. Inst. Mech. Eng. Part D J. Automob. Eng.* **2004**, *218*, 1011–1024. [CrossRef]

14. Huang, Z.H.; Lu, H.B.; Jiang, D.M.; Zeng, K.; Liu, B.; Zhang, J.Q.; Wang, X.B. Engine performance and emissions of a compression ignition engine operating on the diesel-methanol blends. *Proc. Inst. Mech. Eng. Part D J. Automob. Eng.* **2004**, *218*, 435–447. [CrossRef]
15. Kumar, N.; Mathiyazhagan, K.; Sreedharan, V.R.; Kalam, A. *Advancement in Oxygenated Fuels for Sustainable Development: Feedstocks and Precursors for Catalysts Synthesis*; Elsevier: Amsterdam, The Netherlands, 2022.
16. Anand, K.; Sharma, R.P.; Mehta, P.S. Experimental investigations on combustion, performance and emissions characteristics of neat karanji biodiesel and its methanol blend in a diesel engine. *Biomass Bioenergy* **2011**, *35*, 533–541. [CrossRef]
17. Chen, Z.; Wang, L.; Zhang, Q.; Zhang, X.; Yang, B.; Zeng, K. Effects of spark timing and methanol addition on combustion characteristics and emissions of dual-fuel engine fuelled with natural gas and methanol under lean-burn condition. *Energy Convers. Manag.* **2019**, *181*, 519–527. [CrossRef]
18. Gong, C.; Li, Z.; Chen, Y.; Liu, J.; Liu, F.; Han, Y. Influence of ignition timing on combustion and emissions of a spark-ignition methanol engine with added hydrogen under lean-burn conditions. *Fuel* **2019**, *235*, 227–238. [CrossRef]
19. Sayin, C.; Uslu, K.; Canakci, M. Influence of injection timing on the exhaust emissions of a dual-fuel CI engine. *Renew. Energy* **2008**, *33*, 1314–1323. [CrossRef]
20. Nguyen, D.; Stepman, B.; Vergote, V.; Sileghem, L.; Verhelst, S. *Combustion Characterization of Methanol in a Lean Burn Direct Injection Spark Ignition (DISI) Engine*; SAE International: Warrendale, PA, USA, 2019.
21. Li, J.; Gong, C.; Su, Y.; Dou, H.; Liu, X. Effect of Preheating on Firing Behavior of a Spark-Ignition Methanol-Fueled Engine during Cold Start. *Energy Fuel* **2009**, *23*, 5394–5400. [CrossRef]
22. Li, J.; Gong, C.; Su, Y.; Dou, H.; Liu, X. Effect of injection and ignition timings on performance and emissions from a spark-ignition engine fueled with methanol. *Fuel* **2010**, *89*, 3919–3925. [CrossRef]
23. Li, Y.; Gong, J.; Deng, Y.; Yuan, W.; Fu, J.; Zhang, B. Experimental comparative study on combustion, performance and emissions characteristics of methanol, ethanol and butanol in a spark ignition engine. *Appl. Therm. Eng.* **2017**, *115*, 53–63. [CrossRef]
24. Nidhi; Subramanian, K.A. Experimental investigation on effects of oxygen enriched air on performance, combustion and emission characteristics of a methanol fuelled spark ignition engine. *Appl. Therm. Eng.* **2019**, *147*, 501–508. [CrossRef]
25. Li, G.; Zhang, C.; Li, Y. Effects of diesel injection parameters on the rapid combustion and emissions of an HD common-rail diesel engine fueled with diesel-methanol dual-fuel. *Appl. Therm. Eng.* **2016**, *108*, 1214–1225. [CrossRef]
26. Li, Y.; Jia, M.; Liu, Y.; Xie, M. Numerical study on the combustion and emission characteristics of a methanol/diesel reactivity controlled compression ignition (RCCI) engine. *Appl. Energ.* **2013**, *106*, 184–197. [CrossRef]
27. Tao, W.; Sun, T.; Guo, W.; Lu, K.; Shi, L.; Lin, H. The effect of diesel pilot injection strategy on combustion and emission characteristic of diesel/methanol dual fuel engine. *Fuel* **2022**, *324*, 124653. [CrossRef]
28. Liu, J.; Wu, P.; Ji, Q.; Sun, P.; Wang, P.; Meng, Z.; Ma, H. Experimental study on effects of pilot injection strategy on combustion and emission characteristics of diesel/methanol dual-fuel engine under low load. *Energy* **2022**, *247*, 123464. [CrossRef]
29. Li, J.; Zhang, R.; Pan, J.; Wei, H.; Shu, G.; Chen, L. Ammonia and hydrogen blending effects on combustion stabilities in optical SI engines. *Energy Convers. Manag.* **2023**, *280*, 116827. [CrossRef]
30. Huang, H.W.; Zhang, Y. Dynamic application of digital image and colour processing in characterizing flame radiation features. *Meas. Sci. Technol.* **2010**, *21*, 085202. [CrossRef]
31. Huang, H.; Zhang, Y. Flame colour characterization in the visible and infrared spectrum using a digital camera and image processing. *Meas. Sci. Technol.* **2008**, *19*, 085406. [CrossRef]